Applications in Energy and Combustion Science 25 (2026) 100441

Contents lists available at ScienceDirect

Applications in Energy and Combustion Science

journal homepage: www.sciencedirect.com/journal/applications-in-energy-and-combustion-science

Comprehensive characterisation of PM emissions from old and modern boilers using wood and fossil fuels

Kamil Krpec [a,*], Oleksandr Molchanov [a], Lenka Kuboňová [a], Jenn-Kun Kuo [b]

[a] VSB – Technical University of Ostrava, Centre for Energy and Environmental Technologies, Energy Research Centre, 17. listopadu 2172/15, 708 00, Ostrava, Czech Republic

[b] Department of Mechanical and Electro-Mechanical Engineering, National Sun Yat-sen University, Kaohsiung 804201, Taiwan

ARTICLE INFO

Keywords:
Boiler
Combustion
Emissions
Fine particles
Fossil fuels
Biomass

ABSTRACT

In light of the increasing number of decommissioned old small-scale combustion appliances, there is great anticipation for a significant improvement in local air quality. However, even modern appliances emit harmful pollutants, necessitating monitoring and reduction to mitigate their impact on the environment. The study compares particulate matter number and mass concentrations in the flue gas from commonly used boiler types. Low-Pressure Cascade Impactor (DLPI) to determine the mass concentration of individual dust fractions was used, as well as an Electrical Low-Pressure Cascade Impactor (ELPI) and a particle mobility sizer SMPS 3936 (TSI). Beyond appliance design, the type and quality of fuel emerged as significant factors influencing flue gas composition. In addition to particulate matter characteristics, measurements of CO, organic gaseous compounds (OGC), and PMx mass concentrations allowed for the determination of correlations among these pollutants. The highest correlation was observed between CO and OGC, with a coefficient of determination (R^2) value of 0.98 for coal combustion. The feasibility of replacing older stationary combustion appliances with new ones was demonstrated across several parameters, including specific emissions for the PM2.5 and PM0.1. The reduction between overfire and automatic boilers reached 99.96 % and 93 %, respectively.

1. Introduction

Total PM10 and PM2.5 emissions decreased noticeably in the EU between 2007 and 2018 (by 21.1 % for PM10 and 22.5 % for PM2.5). However, emissions of particulate matter from the combustion of solid fuels in small stationary sources declined less during the same period - by 11.8 % for PM10 and 9.6 % for PM2.5 [1]. In the Czech Republic, residential stationary sources accounted for 57.2 % of total PM10 emissions and 74.1 % of total PM2.5 emissions in 2016 [2]. Common solid fuels used in local residential stationary sources, not only in the Czech Republic [3] but across the entire EU, include wood, coke, wood pellets, and black and brown coal. For example, in 2017, the domestic energy sector was identified as an important contributor to the global burden of PM2.5-related disease [4]. Emission estimates for this sector still carry high uncertainty, mainly due to a lack of reliable activity data and limited understanding of end-user behaviour [5], especially compared with the industrial sector.

Combustion processes are among the most significant sources of air pollution. Particulate matter (PM) is a key pollutant, not only due to its deposition in the respiratory tract, but also because of the sorption of other flue gas components onto particle surfaces, such as PAHs, PCDD/PCDFs, PCBs, and others. These pollutants are produced not only by the combustion of fossil fuels but also by biomass combustion. It has been confirmed that biomass combustion also produces soot [6]. The fact that biomass combustion is not emission-free complicates the planned transition away from fossil fuels. Several studies have highlighted potential health risks associated with wood burning [7]. Stricter legislative regulations for biomass combustion in the domestic heating sector may therefore be expected in the coming years.

From the perspective of human health impacts of atmospheric aerosols—solid, liquid, or mixed particles suspended in the atmosphere—particle size fractions, referred to as PMx, have been defined to include particles smaller than x μm in aerodynamic diameter. Particle size is a key factor determining the behaviour and deposition of particles within the respiratory system [8–10]. Factors such as air excess, fuel properties, operator behaviour, and the type of combustion device

* Corresponding author.
E-mail addresses: kamil.krpec@vsb.cz (K. Krpec), oleksandr.molchanov@vsb.cz (O. Molchanov), lenka.kubonova@vsb.cz (L. Kuboňová), jenn.kun@mail.nsysu.edu.tw (J.-K. Kuo).

https://doi.org/10.1016/j.jaecs.2025.100441
Received 15 August 2025; Received in revised form 1 December 2025; Accepted 3 December 2025
Available online 5 December 2025

significantly influence PMx formation [11–14]. Nevertheless, it has been observed that particles smaller than 1 μm constitute the majority of particles in flue gas from biomass combustion [15–18].

Numerous studies have investigated PM emissions from residential heating systems, with most research focused on single boiler types or limited fuel comparisons at nominal operating conditions [19,20], which poorly represent real-world operation. However, real-world operation often involves reduced heat output due to improved building insulation or frequent load changes and cold starts. These conditions significantly alter combustion dynamics, thus significantly differ from standard testing protocols. Furthermore, previous studies have primarily emphasised PM2.5 and PM1 fractions, with limited attention to ultrafine particles (PM0.1).

The harmful particulate matter (PM) emissions from residential heating were recently suggested to be solved through several emission control technologies, including electrostatic precipitation [21,22] catalytic treatment [23,24] and a novel approach involving AI-based predictive modelling of the combustion process [25]. However, these measures do not fully address the variability in emissions caused by different combustion technologies and fuel types; thus, a fundamental question remains: what emission reductions are practically achievable through direct technology replacement? This is particularly relevant as many European countries implement boiler replacement programs without comprehensive data on the actual benefits across different fuel types and operating conditions.

Recent studies have made important contributions: Johansson et al. [19] characterised emissions from wood combustion at nominal output, Mack et al. [26] evaluated modern pellet systems, and Křůmal et al. [27] compared gaseous pollutants from various boilers. However, these studies did not provide: (1) comprehensive simultaneous characterisation of both mass and number concentrations across the full particle size spectrum, (2) systematic quantification of emission reductions achievable through technology replacement under realistic operating conditions, or (3) high temporal resolution data capturing the combustion processes' dynamics.

This manuscript addresses these gaps by presenting a comprehensive investigation of PM emissions from four boiler technologies spanning from obsolete overfire designs (class 1) to state-of-the-art automatic systems (class 5), operated with five different fuel types under realistic reduced-load conditions. Our specific objectives were to:

1. Quantify mass and numerical concentrations of fine (PM2.5, PM1) and ultrafine (PM0.1) particles using multiple high-resolution measurement techniques (HR-ELPI+, SMPS, DLPI)
2. Establish correlations between gaseous pollutants (CO, OGC) and PM formation for different fuel types, providing insights into combustion quality indicators.
3. Determine specific emission factors under reduced heat output (~50 % nominal) representing real-world operation.
4. Provide quantitative evidence for the emission reduction potential of boiler replacement programs, with particular emphasis on ultrafine particle fractions.

Unlike previous studies that typically examined single aspects of this problem, we present an integrated dataset enabling direct comparison across the full spectrum of residential heating technologies currently in use across Central Europe.

Specific emissions (SE) of gaseous compounds, as well as mass and number concentrations of PMx, were calculated for the overfire boiler (B1), the down-draft combustion boiler (B2), the gasification boiler (B3), and the automatic boiler (B4). Older boiler designs were selected for the experiments because, although their replacement with modern technologies (e.g., pellet boilers) has begun, traditional appliances remain widely used.

2. Materials and methods

2.1. Fuel parameters determination

The proximate and ultimate analyses (Table 1), along with the net calorific values (NCV), were determined for the following fuels: dry spruce wood (DW), wet spruce wood (WW), brown coal (BC), brown coal briquettes (BCB), and hard coal (HC).

The fuel moisture was determined in accordance with EN ISO 18134–2:2017 [28]. The ash was determined according to the procedure specified in ISO 1171:2010 [29] and EN ISO 18122:2015 [30]. The ultimate analysis was measured by LECO CHNS628 analysers according to ISO 29541:2010 [31] and EN ISO 16948:2015 [32], and analysis of S according to standards ISO 19579:2006 [33] and ISO 16994:2016 [34]. The gross and net calorific values were determined according to standards ISO 1928:2010 [35] and ISO 18125:2017 [36].

2.2. Combustion devices

Four different designs of hot-water boilers were used for the experiments. Boiler B1 (class 1, certified fuels – wood, coke, black coal, nom. heat output 22–30 kW) is a representative of the oldest types of boilers, which are currently being replaced by more modern boilers. It is equipped with a combustion chamber into which the entire batch of fuel is fed, which gradually burns out. Above the combustion chamber is a small heat exchanger; below it is a space for the resulting ash. The boiler has any fireclay lining. B2 boiler (class 2, certified fuel – brown coal, nom.heat output 32 kW, represents a more modern design of boilers with manual fuel addition, where the fuel storage is separated from the combustion chamber and only a certain part of the fuel burns in the boiler, which leads to better control of the combustion process and lower production of pollutants. Fireclay bricks are placed in the combustion chamber and secondary combustion air is introduced into it. B3 boiler (class 3, certified fuels – brown coal, wood, nom.heat output 20 kW) is a representative of the most modern construction of boilers with manual fuel addition. The fuel is gradually gasified in the fuel storage. A nozzle with a secondary combustion air supply is located between the fuel storage and the combustion chamber. The resulting gas burns in a thermally insulated combustion chamber. The B4 boiler (class 5, certified fuel – brown coal, wood pellets, nom.heat output 25 kW) is a modern automatic boiler, equipped with an external fuel tank, from which the fuel is transported to the retort burner using a screw conveyor. Combustion air is supplied to the burner, a fireclay deflector is placed above the burner. The boiler is equipped with a modern control unit.

Boilers diagrams are in our previous publication [27].

2.3. Measuring apparatus of gaseous compounds of flue gas

Flue gas was sampled at a flow rate of 2.0 L/min just behind the boilers at the sampling point "SP1" (Fig. 1). The sampling system consisted of a heated filter (180 °C) for dust separation and a heated

Table 1
Analysis of used fuels.

Fuel	NCV MJ/kg	C % wt	H % wt	S % wt	N % wt	O % wt	Moisture %wt	Ash % wt
WW	10.0	29.7	3.79	ND	0.05	26.0	40.10	0.32
DW	16.6	45.4	5.79	ND	0.08	39.7	8.48	0.49
BC1 (B1, B2, B3)	18.6	48.7	3.88	0.89	0.71	11.7	29.4	4.75
BC2 (B4)	21.2	54.9	4.33	0.95	0.67	12.8	18.7	7.61
BCB (B1, B2)	19.0	52.1	3.99	0.48	0.53	19.5	18.6	4.78
HC1 (B2)	28.2	71.5	4.89	0.59	1.39	9.11	4.93	7.61
HC2 (B4)	24.3	62.8	4.17	1.01	1.03	11.0	11.5	8.47

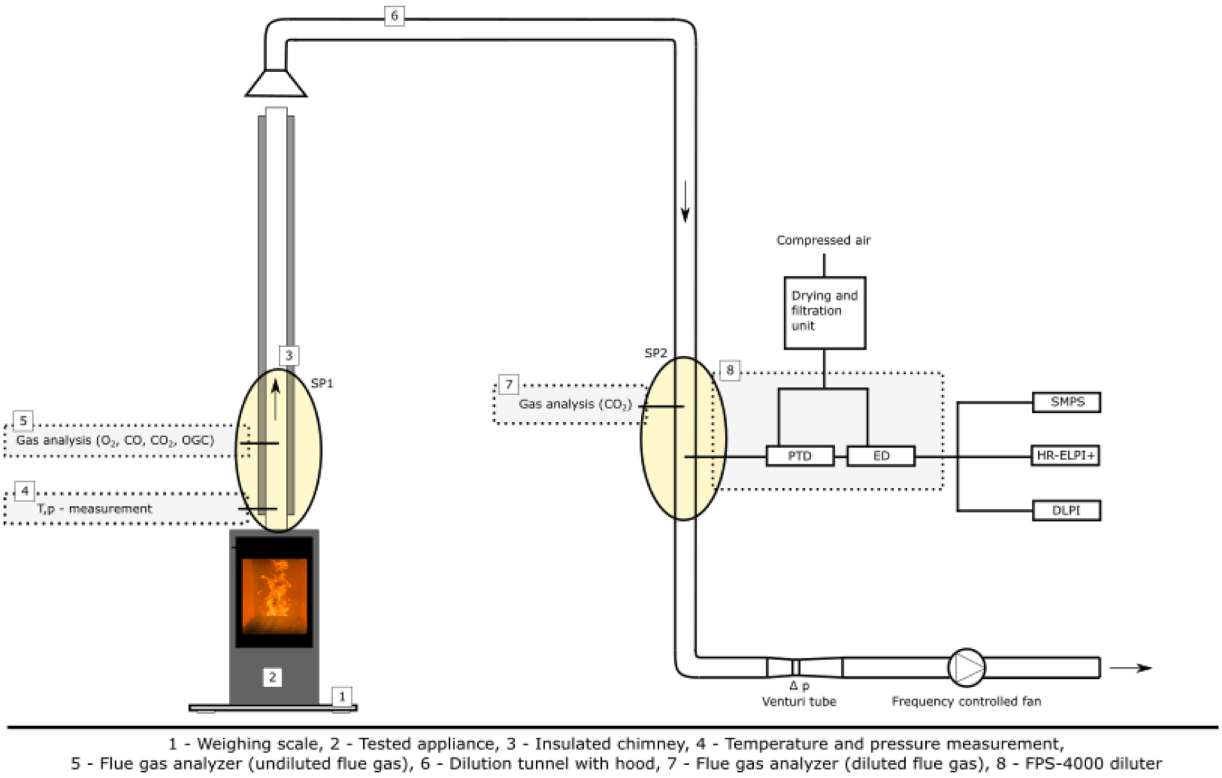

Fig. 1. Measuring system.

sampling line (180 °C). Then the flue gas sample was separated – the first part was directed to the OGC analyser (MultiFID14, ABB), and the second part was cooled to 3 °C in the M&C cooler, filtered, and analysed in a set of analysers. CO, CO_2 was detected by NDIR analysers (URAS26, ABB) and O_2 was detected by a paramagnetic analyser (Magnos 206, ABB). The NDIR analysers offered an accuracy of ±1.5% for concentrations ranging from 0 to 5,000 ppm or 0 to 100,000 ppm for CO and from 0 to 20% for CO_2.

Nitrogen oxides were measured using a Horiba PG-350E chemiluminescence analyser (CLA) equipped with a NOx converter. The measurement accuracy was better than ±1.5 % over the 0–500 ppm range.

The dilution ratio in the dilution tunnel (sampling point „SP2“) was calculated from data from the NDIR CO_2 analyser (GMP343, Vaisala).

For the calculation of the dilution ratio of the dilution tunnel, the following equation was used:

$$DR(DT) = (CO2, SP1 - CO2, ambient)/(CO2, SP2 - CO2, ambient) \quad (1)$$

Here, DR (DT) is the dilution ratio of the dilution tunnel, CO2,SP1 is CO_2 concentration measured behind the boiler, CO2,ambient is CO_2 concentration in ambient air (averaged value from the concentration measured before and after of each experiment – measured by Vaisala analyser), CO2,SP2 is CO_2 concentration measured in the dilution tunnel.

2.4. Measurement line and PM collection equipment

Above the chimney, the dilution tunnel digester was installed in accordance with EPA Method 5 G [37]. PM sampling was conducted in a dilution tunnel at the sampling point „SP2“ (Fig. 1).

To avoid clogging and condensation in downstream equipment and to ensure compatibility with operational requirements, an additional dilution - the Dekati FPS-4000 two-stage diluter was implemented at the "SP2″ sampling point. The FPS-4000 dilution system provides sufficient diluted flue gas for connecting various PM measuring devices simultaneously. The first dilution step in the FPS-4000 diluter is done by the perforated tube diluter, and the second step is done by the ejector diluter. Dilution air is filtered by a HEPA filter. The whole system was controlled by the original Dekati SW, which also calculates the actual final dilution ratio.

Two on-line PM measurement instruments were used for PM number size distribution determination – High Resolution Electrical Low Pressure Impactor (HR-ELPI+, Dekati Ltd.) and a SMPS 3936 (TSI Inc.).

HR-ELPI+ was operated in high-resolution mode, in which up to 500 PM size classes were determined using Dekati's original data analysis software at a sampling frequency of 1 Hz. The flow of the sample through the HR-ELPI+ was 10 L/min. Sintered collection plates were used at each physical impactor stage. As the final stage of the impactor, the backup filter was used.

Used SMPS, consisted of CPC (model 3775, TSI Inc.) and EC (model 3080, TSI Inc.) with a long DMA (model 3081, TSI Inc.), and an aerosol neutraliser (model 3077A, Kr-85, 10 mCi, TSI Inc.). SMPS was equipped with a 0.071 cm jet size impactor. The SMPS settings are described in our previous study [38].

For the mass determination of individual PM fractions, a 13-stage Low Pressure Impactor (DLPI, Dekati) was used. The Impactor was operated at a flow of 30 L/min. Greased (Apiezon-L grease) aluminium foils were used as a collection substrate. The bounce effect must be taken into account when using the impactor, so the producer's instructions about the maximal particle mass deposited on each stage were followed. The actual cut-off diameters were calculated based on the flow velocity, viscosity, and mean free path corresponding to the stagnation conditions [39]. The cut-off diameter of the impactor could vary when the inlet pressure and temperature differed from the calibration conditions [40], so the temperature and pressure inside the impactor were measured and considered during evaluation of the results. An analytical laboratory microbalance with 0.001 mg resolution (Mettler Toledo XP6) was used to weigh aluminium foils before and after sampling. Before weighing, the static charge on aluminium foils was neutralised using an antistatic frame.

2.5. Quality control measures

Before each experimental series, all gas analysers were calibrated. Calibration procedures included zero calibration with ultra-high-purity nitrogen (99.999 %) and span calibration with certified reference gases (SIAD) for CO, CO_2, and NOx. The span calibrations of O_2 were done by using ambient air.

To reduce particle measurement errors introduced by the dilution system, ambient air was pre-filtered with a HEPA filter, reducing background particle concentrations to below 200 particles/cm^3. The actual dilution ratio was verified by comparing CO_2 concentrations in the raw flue gas and diluted sample within the mixing chamber. The dilution ratio was settled at 1:80 and verified by comparing the CO_2 concentrations in the flue gas and the sample; the dilution uncertainty was approximately ±5%.

All particle sampling was conducted isokinetically, with probes positioned at the centreline of the flue gas duct. The sampling location was in a straight, horizontal section of the duct with a constant diameter of 150 mm, at least five duct diameters from any bends or disturbances, and within ±15% of isokinetic tolerance. This setup complies with the requirements of EN 13284–1:2017.

Data normalisation and evaluation

Concentrations of combustion gases and particulate matter were standardised to a dry gas volume at 101.325 kPa, 0 °C, and a reference oxygen (O_2) level of 10 % and then recalculated to SE.

Particle number (PN) concentration data are reported as total number concentration and as differential concentrations, expressed as dN/dlog(Dp). Here, dN represents the particle count within each size bin, and dlog(Dp) denotes the logarithmic width of each particle diameter range. This format enables consistent comparisons across instruments with varying binning configurations.

3. Results and discussion

3.1. Parameters of combustion tests

In total, 14 experiments were conducted mostly with 3 repetitions per experiment. The averaged measured boiler output, flue gas temperatures at sampling points SP1 and SP2 (TSP1, TSP2), oxygen at sampling point SP1 (O2SP1), and the dilution ratios are presented in Table 2 and Table 3. The boilers were connected to the chimney in accordance with testing standard EN 303–5. Boilers reached stable operating conditions before the start of the combustion experiments. Boilers B1-B3 were operated as follows: the duration of this initial period was at a minimum of 2 h and was sufficient for establishing a necessary basic fire bed in the boiler [41]. Thus, the initial period was not included in the collected samples in all measured boilers. After the initial period, the fuel was added in the amount equal to 60 % of nominal output, and the boilers were operated at reduced heat output by the regulation of the combustion air supply or flue gas fan (boiler B3). The fan was turned off for most of the combustion test. The combustion experiments began by adding the fuel to the combustion chamber in accordance with the EN 303–5 testing standard. The experiments finished on approximately the same basic fire bed in the boiler. The goal was to operate the boilers (B1-B3) at approximately 50 % of nominal output. It was not possible to reach this output with the WW for B1 and B2, even with fully opened combustion air. For boiler B2, achieving 50 % of the nominal output proved very difficult when burning all fuels except BC1. Boiler B4 was pre-heated for about 1,5 h with the heat output set to minimal heat output (30 % of the nominal heat output, controlled by the control unit). Then started the sampling period.

Table 2
Parameters of combustion tests (WW, DW).

Combustion test		B1-WW	B2-WW	B3-WW	B1-DW	B2-DW	B3-DW
Combustion device		B1	B2	B3	B1	B2	B3
Fuel		WW	WW	WW	DW	DW	DW
Output	kW	6.1	4.4	11.0	11.1	9.9	13.1
Output	%	30.3	13.8	43.8	55.3	31	52.5
TSP1	°C	153	107	196	241	227	172
TSP2	°C	50.3	27.3	49.8	46.5	39.2	32.9
O2SP1	vol. %	18.2	16.7	15.3	13.7	13.4	12.3
Dilution ratio DT	-	4.0	12.4	5.7	8.1	9.6	10.2
Dilution ratio FPS	-	159	42.9	94.1	93.1	47	44.6
Total DR	-	639	534	537	754	451	453

3.2. Specific emissions of CO, OGC and PMx

Table 4 and Table 5 (heatmap versions presented as Table T1 and Table T2 in supplementary materials) show SE of OGC, CO and PMx. When burning WW and DW, SE CO values ranged from about 4,800 mg/MJ to 8,900 mg/MJ, and SE OGC values ranged from 1,000 to 3,100 mg/MJ. Another study [19] reported comparable SE values for birch wood combustion, even when boilers were operated only at nominal heat output. Another study [20] also reported very similar results for an up-draft boiler (B1-like boiler) with dry (8 % moisture) acacia and larch wood. Boiler B3 always achieved the best results; however, SE CO were lower compared to the worst boiler by only approximately 31 % (WW) or 23 % (DW). In the case of SE OGC, the difference between B3 and the boiler with the highest SE was 48 % for both DW and WW. The high SE of CO and OGC for the relatively modern B3 boiler can be explained by operation at reduced power with the fan off. In a previous study [19], SE values were <1,000 mg/MJ (CO) or <60 mg/MJ (OGC) when burning wood with a moisture content up to 26 % (rated output). When burning wood with a moisture content of 38 %, there was a substantial increase in SE CO to 3,700 mg/MJ and OGC 690 mg/MJ, and this increase was also observed in our tests. Some studies show that the emissions produced depend on how the fuel is ignited in the boiler. E.g. Kraszkiewtz [42] burned pine wood in a boiler of similar design to B1, however, the SE CO values, both with top-down ignition and bottom-up ignition, were again similar to ours (principally top-down ignition of the fuel batch).

For BC1 combustion, SE CO and OGC values for boilers B1 and B2 were higher than during DW or WW combustion. Lower SE of CO and OGC were observed for boiler B3 (in the case of OGC, SE was reduced by up to three times). When burning BCB (boiler B1, B2), SE CO values were approximately 2 times lower than for BC combustion, and SE OGC values were approximately 2–4 times lower. During the combustion of HC1 in boiler B2, the value of SE CO was at a level similar to that during combustion of BC1, but the value of SE OGC was approximately 2.7 times higher. Combustion of both HC2 and BC2 in boiler B4 was accompanied by the absolute lowest SE of CO and OGC. Our results are in good agreement with the study [43], which tested two coal burners in a class 5 boiler with HC. At nominal heat output, SE CO was similar to ours; SE OGC was 4 times higher with the standard retort burner, while with the innovated burner, SE OGC was 2 times lower than ours. At reduced heat output, SE CO was about 2 times higher, and SE OGC was 3 times higher. Even though the B4 boiler (class 5, state-of-the-art boiler) achieved the lowest SE CO and OGC, the measured values are still higher than those for modern pellet-fired boilers. E.g., the Mack [26] shows that with the most modern wood pellet boilers (drop-down burner), SE CO values <5 mg/MJ can be achieved (approx. 50 times lower than when burning HC in B4), while SE OGC values were <1 mg/MJ. Pellet stove was also measured in the mentioned study, while the SE CO and OGC values corresponded to the values measured on the B4 boiler. However, for pellet boilers, it depends heavily on the burner and combustion chamber design. Pelka [44] shows that the values of SE CO and OGC

Table 3
Parameters of combustion tests (BC, BCB, HC).

Combustion test		B1-BC1	B2-BC1	B3-BC1	B4-BC2	B1-BCB	B2-BCB	B2-HC1	B4-HC2
Combustion device		B1	B2	B3	B4	B1	B2	B2	B4
Fuel		BC1	BC1	BC1	BC	BCB	BCB	HC1	HC2
Output	kW	11.4	13.2	13.0	7.1	18.7	11.1	10.7	8.0
Output	%	50.5	41.3	51.9	28.2	83	34.6	33.4	32.0
TSP1	°C	178	195	212	68.0	266	183	173	84.0
TSP2	°C	28.1	31.9	38.1	23.6	45.8	29.4	30	24.7
O2SP1	vol. %	7.4	7.3	10.6	11.8	7.4	8.6	10.2	10.1
Dilution ratio DT	-	16.3	13.8	11.7	22.4	9.1	16.2	14.8	22.5
Dilution ratio FPS	-	166.4	74.7	36.9	12.0	137.8	46.4	86.6	12.0
Total DR	-	2,706	1,032	433	268	1,250	754	1,285	270

Table 4
SE of gaseous compounds and particle mass concentrations (WW, DW).

Combustion test		B1-WW	B2-WW	B3-WW	B1-DW	B2-DW	B3-DW
Combustion device		B1	B2	B3	B1	B2	B3
Fuel		WW	WW	WW	DW	DW	DW
SE CO	mg/kg	75,813 ± 4,187	102,367 ± 6,300	62,109 ± 11,297	97,934 ± 15,455	83,362 ± 13,040	79,392 ± 9,863
SE OGC	mg/kg	27,054 ± 1,852	36,015 ± 5,004	16,419 ± 5,571	29,692 ± 9,102	19,670 ± 7,701	16,254 ± 2,173
SE NOx	mg/kg	503 ± 94	601 ± 42	592 ± 77	989 ± 189	889 ± 63	653 ± 21
SE SO2	mg/kg	N/A	N/A	N/A	N/A	N/A	N/A
SE PM2.5	mg/kg	7,693 ± 661	4,457 ± 730	2,369 ± 1,384	5,464 ± 2,933	2,185 ± 441	754 ± 229
SE PM1	mg/kg	7,679 ± 661	4,446 ± 730	2,364 ± 1,380	5,453 ± 2,931	2,172 ± 442	750 ± 227
SE PM0.1	mg/kg	1,463 ± 215	394 ± 158	516 ± 207	1,185 ± 580	374 ± 11	149 ± 49
SE CO	mg/MJ	7,801 ± 431	8,891 ± 547	6,191 ± 1,126	6,182 ± 976	5,014 ± 784	4,775 ± 593
SE OGC	mg/MJ	2,784 ± 191	3,128 ± 435	1,637 ± 555	1,874 ± 575	1,183 ± 463	978 ± 131
SE NOx	mg/MJ	52 ± 10	52 ± 4	59 ± 8	62 ± 12	53 ± 4	39 ± 1
SE SO2	mg/MJ	N/A	N/A	N/A	N/A	N/A	N/A
SE PM2.5	mg/MJ	792 ± 68	387 ± 63	236 ± 138	345 ± 185	131 ± 26	45 ± 14
SE PM1	mg/MJ	790 ± 68	386 ± 63	236 ± 138	344 ± 185	131 ± 27	45 ± 14
SE PM0.1	mg/MJ	151 ± 22	34 ± 14	51 ± 21	75 ± 37	23 ± 1	9 ± 3

Table 5
SE of gaseous compounds and particle mass concentrations (BC1, BC2, BCB, HC1, HC2).

Combustion test		B1-BC1	B2-BC1	B3-BC1	B4-BC2	B1-BCB	B2-BCB	B2-HC1	B4-HC2
Combustion device		B1	B2	B3	B4	B1	B2	B2	B4
Fuel		BC1	BC1	BC1	BC2	BCB	BCB	HC1	HC2
SE CO	mg/kg	418,968 ± 124,361	253,793 ± 40,316	67,968 ± 27,715	4,679 ± 2,423	264,257 ± 21,267	112,764 ± 39,881	99,623 ± 38,893	4,004 ± 123
SE OGC	mg/kg	90,981 ± 26,197	63,341 ± 6,192	6,204 ± 5,533	97 ± 33	54,045 ± 6,474	16,561 ± 10,621	22,918 ± 20,690	70 ± 34
SE NOx	mg/kg	1,276 ± 123	1,474 ± 281	2,745 ± 393	4,275 ± 300	976 ± 80	1,366 ± 149	3,531 ± 84	4,607 ± 124
SE SO2	mg/kg	9,663 ± 454	12,030 ± 300	11,849 ± 1,969	10,871 ± 1,233	4,027 ± 334	2,905 ± 410	9,410 ± 1,273	15,626 ± 350
SE PM2.5	mg/kg	68,239 ± 34,427	16,784 ± 1,981	548 ± 344	271 ± 101	6,249 ± 3,424	876 ± 589	5,254 ± 3,632	1,106 ± 253
SE PM1	mg/kg	67,073 ± 33,551	16,711 ± 1,891	527 ± 323	262 ± 106	6,227 ± 3,406	865 ± 593	5,089 ± 3,588	1,089 ± 249
SE PM0.1	mg/kg	1,443 ± 483	415 ± 61	173 ± 72	95 ± 29	506 ± 213	177 ± 76	363 ± 150	344 ± 64
SE CO	mg/MJ	22,586 ± 6,704	13,682 ± 2,173	3,261 ± 1,330	235 ± 122	13,907 ± 1,119	5,934 ± 2,099	3,533 ± 1,379	165 ± 5
SE OGC	mg/MJ	4,905 ± 1,412	3,415 ± 334	298 ± 265	5 ± 2	2,844 ± 341	872 ± 559	813 ± 734	3 ± 1
SE NOx	mg/MJ	69 ± 7	79 ± 15	132 ± 19	214 ± 15	51 ± 4	72 ± 8	125 ± 3	190 ± 5
SE SO2	mg/MJ	521 ± 24	649 ± 16	569 ± 94	545 ± 62	212 ± 18	153 ± 22	334 ± 45	644 ± 14
SE PM2.5	mg/MJ	3,679 ± 1,856	905 ± 107	26 ± 17	14 ± 5	329 ± 180	46 ± 31	186 ± 129	46 ± 10
SE PM1	mg/MJ	3,616 ± 1,809	901 ± 102	25 ± 15	13 ± 5	328 ± 179	46 ± 31	180 ± 127	45 ± 10
SE PM0.1	mg/MJ	78 ± 26	22 ± 3	8 ± 3	5 ± 1	27 ± 11	9 ± 4	13 ± 5	14 ± 3

measured in pellet boilers can be only 2–5 times lower than those measured by us when burning coal. It can be assumed that very cheap pellet boilers can have parameters comparable to, or even worse than, those of a B4 coal-burning boiler. When burning wood, boiler B1 achieved lower SE than when burning fossil fuels. Boiler B2 achieved better SE values only when burning HC1, when burning BCB SE values were comparable to those for DW, and when burning BC, SE values were even higher than SE values for WW. For boiler B3, SE CO and OGC values were lower for BC1 combustion than for WW and DW combustion. It is known that CO and OGC emissions depend mainly on the method of supplying combustion air to the fuel, and further on whether the combustion plant is equipped with a secondary combustion air supply. SE OGC also significantly affects whether the combustion chamber of the boiler is sufficiently insulated, i.e. whether the temperature in the hearth is sufficiently high.

The clear relationship between combustion chamber design and emissions was confirmed by our results (please see Table 4 and Table 5): burning DW, WW and BC, the lowest OGC values (298–1,637 mg/MJ) were consistently achieved for the B3 boiler compared to the other boilers with manual fuel loading, including B1 with the OGC content of 872–4,905 mg/MJ. Notably, both boilers have similar CO levels, suggesting that the difference in OGC emissions is due to factors other than CO production. This can be attributed to higher combustion temperatures (>1,000 °C) in the insulated chamber, which was stated by numerous studies, including Nussbauner et al. [45], promoting complete oxidation of volatile organic compounds, in which they are fully burned into simpler compounds like carbon dioxide and water, reducing the release of unburned or partially burned compounds. Also, higher combustion temperatures in B3 make soot precursors more likely to react with oxygen and decompose, leading to reduced soot emissions rather than aggregating into larger soot particles [46]. This is supported by data from HR-ELPI+ (please see Figures S6-S8), demonstrating in Boiler B3's emissions the lower content of particles in accumulation-mode (larger than 100 nm): since these particles typically form when organic vapours condense into solid forms, the reduced presence of such particles in B3 indicates less condensation, which aligns with the lower OGC emissions observed.

The volatile combustible content of the fuel also affects SE OGC. E.g. the Knigawka [47] showed that by using so-called smokeless coal with a 3–7 times lower volatile combustible content, compared to HC, there was a 6–70-fold reduction in SE OGC. Another way to reduce CO and OGC emissions is the use of catalytic converters. Our previous study [48] shows that when burning wood, a CO conversion rate in the range of 70–90 % can be achieved, depending on the type of material used. In the case of OGC, the conversion rate was lower, only about 25 %. Close to linear correlation between the SE OGC and the SE CO for combustion tests with coal was found - $R^2 = 0.98$ (Fig. 2), but no general correlation was found for wood ($R^2 = 0.67$). Our findings regarding the correlation between CO and OGC from wood burning contradict an earlier study [19] that reported a correlation. Another study [26] found a significant correlation between CO and OGC (R^2=0.99), but in this case, wooden pellets were burnt in a wood stove.

The SO_2 and NOx contents in the flue gas (see Table 4 and Table 5) are primarily determined by the sulfur and nitrogen contents of the fuel (see Table 1). This relationship was presented in our previous study [27].

3.3. Average SE – particle mass concentration

The SE of PM1 has been observed in previous studies, where the values varied from 9 to 613 mg/MJ for biomass combustion [49,50], depending on the type of combustion device used and the type of biomass. The experiments we conducted can be divided into two main groups based on the type of fuel used - biomass or fossil fuels. When burning DW, the highest SE PM2.5 was found for boiler B1, namely 345 mg/MJ. On the other hand, the lowest SE PM2.5 was measured for boiler B3 – 45 mg/MJ (approx. 8 times lower than in boiler B1). This difference fully corresponds to the age of the construction of both boilers. The SE PM2.5 value of 131 mg/MJ was measured for boiler B2, which is 3 times lower than for boiler B1. When burning WW, the highest SE PM2.5 value was again measured for boiler B1 – 792 mg/MJ and the lowest for boiler B3 – 236 mg/MJ (3 times lower). For boiler B1, PM2.5 SE increased 2 times during WW combustion (compared to DW combustion), while SE increased 5 times for boiler B3. For boiler B2, SE increased 3 times. For

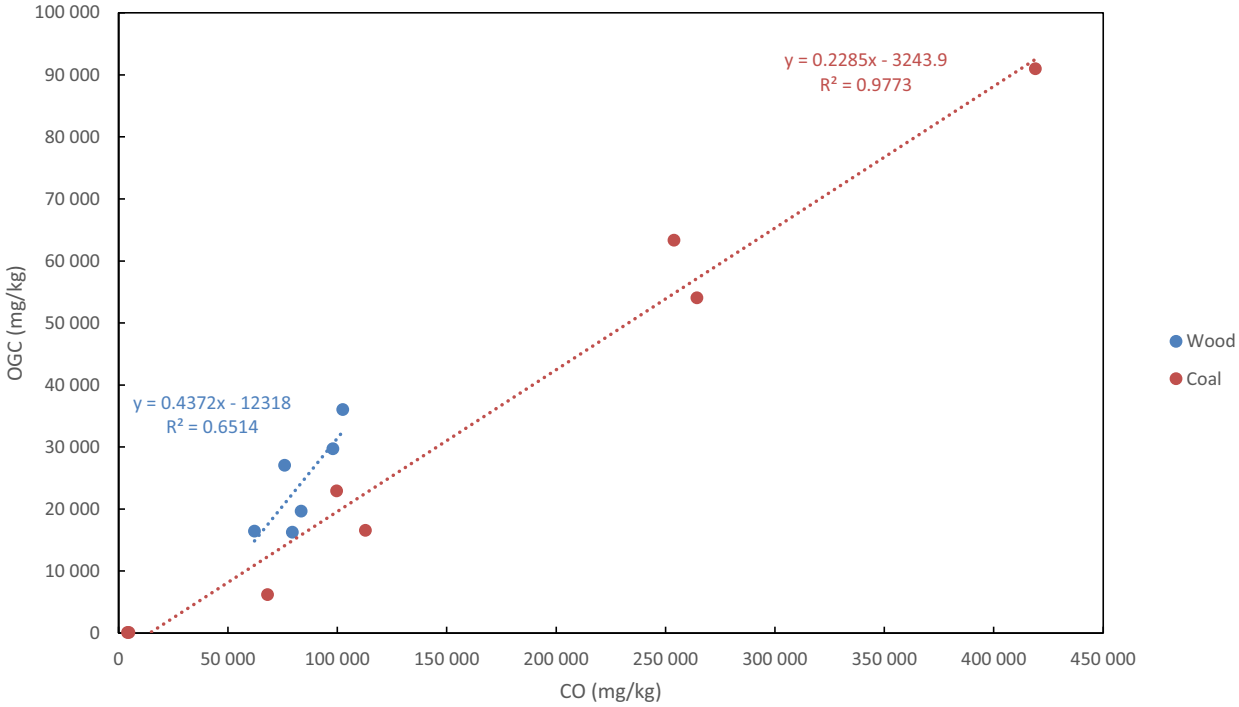

Fig. 2. The correlation between the SE OGC and SE CO.

the boilers we tested, it appears that more modern boiler designs show a greater dependence of PMx production on the quality (moisture) of the biomass being burned than older boiler designs. However, even when burning wet wood, the modern boiler (B3) achieved SE PM2.5 values 1.5 times lower than those of boiler B1 when burning dry wood.

During BC combustion, the highest SE PM2.5 was measured for boiler B1, at 3,679 mg/MJ. On the contrary, the lowest SE was measured for boilers B4 and B3 – 14 and 26 mg/MJ, respectively, which are approximately 185 times lower than the highest SE. BCB fuel was burned only in boiler B1 and B2, because the other boilers do not allow the burning of this fuel due to design reasons. A value of 46 mg/MJ was measured for boiler B2, which is 7 times lower than the value measured for boiler B1. In both boilers, there was a significant reduction in SE PM2.5 when burning BCB compared to burning BC (20 times for boiler B2, 11 times for boiler B1). HC fuel was burned in boilers B4 and B2, while boiler B4 had approximately 4 times lower SE PM2.5 (46 mg/MJ) than boiler B2. At the same time, the B4 boiler had an SE that was 3 times higher than when burning BC fuel. For boiler B2, the measured SE value was 5 times lower than when burning BC1, but it was also 4 times higher than when burning BCB, and 1.4 times higher and 2 times lower than when burning DW and WW, respectively. When burning BC1, boiler B3 SE had PM2.5 approximately 2 times lower than when burning DW and 9 times lower than when burning WW. From the measured results, it can be seen that modern boilers achieve low SE PM2.5 values even when SE CO and OGC are relatively high. For example, the tests B3-DW and B3-BC1 can be mentioned. SE PM2.5 was also low for boiler B4. The surprise was the B2-BCB test, where the SE PM2.5 value was comparable to the B4-HC2 test.

Fig. 5 shows the distribution of particles according to their mass size fractions during the combustion of DW and WW. It can be seen that PM1 accounts for more than 97 % of PM10, with PM0.1 accounting for an average of 20 % of total PM. Only when burning WW in boiler B2 was a lower PM0.1/PM10 ratio measured, i.e., 8 %. When burning BC, BCB and HC (Fig. 6), the representation of PM1 in PM10 was in the range of 95–98 %, which is approximately the same level as when burning wood. For PM0.1, the values ranged from 3–35 % of PM10, with the lowest values measured for boilers B1 and B2 burning BC (i.e. poor combustion process), while the highest values were measured for boilers B3 and B4 burning BC and for boiler B4 during HC combustion (i.e. with a good combustion process). Our findings are in good agreement with previous studies, where PM1 in average included of about 90 % of total PM [51, 52].

The correlation coefficient R^2 is 0.71 for coal combustion and 0.07 for biomass combustion (Fig. 3), indicating no linear relationship between CO and PM2.5.

The R^2 coefficient for coal combustion was 0.58 and 0.48 for wood combustion for the correlation of PM2.5 and OGC (Fig. 4).

3.4. PN concentrations

Averaged numerical size concentrations of particles divided into two size classes, namely particles up to 0.1 μm in size and particles up to 0.8 μm (the maximum size measured by the SMPS device), are shown in Table 6 (heatmap versions presented as Table T3 in supplementary materials) . Fine emitted particles are PM1, ultrafine emitted particles are PM0.1 [53]. A previous study [54] shows that fine particles produced during optimal biomass combustion have greater toxicological potential than those emitted during poor combustion. Generally, the toxicity of PM, which is released during solid fuel combustion—namely coal, wood, and biomass, leads to premature mortality, comparable to that of wars and violence before 2015 [55]. The toxicity of PM0.1 poses significant health risks due to its ability to penetrate deep into the lungs, thus leading to severe respiratory health issues, including asthma and chronic obstructive pulmonary disease (COPD), as well as cardiovascular risks, including heart attacks and strokes, due to the inflammation and oxidative stress it causes. It most affects vulnerable populations such as children and the elderly [56]. The toxicity of PM0.1 particles is the subject of many studies, and it has been shown [57] that the presence of particle-bound PAHs contributes significantly. Samae et al. demonstrated [58], that PM0.1 contains approximately seven times more particle-bound PAHs in the case of bituminous coal combustion than in biomass combustion. However, Sikorova et al. in a more recent study [59] showed, that the technology of the boilers was a more important factor in determining the genotoxic potential than the fuels burned.

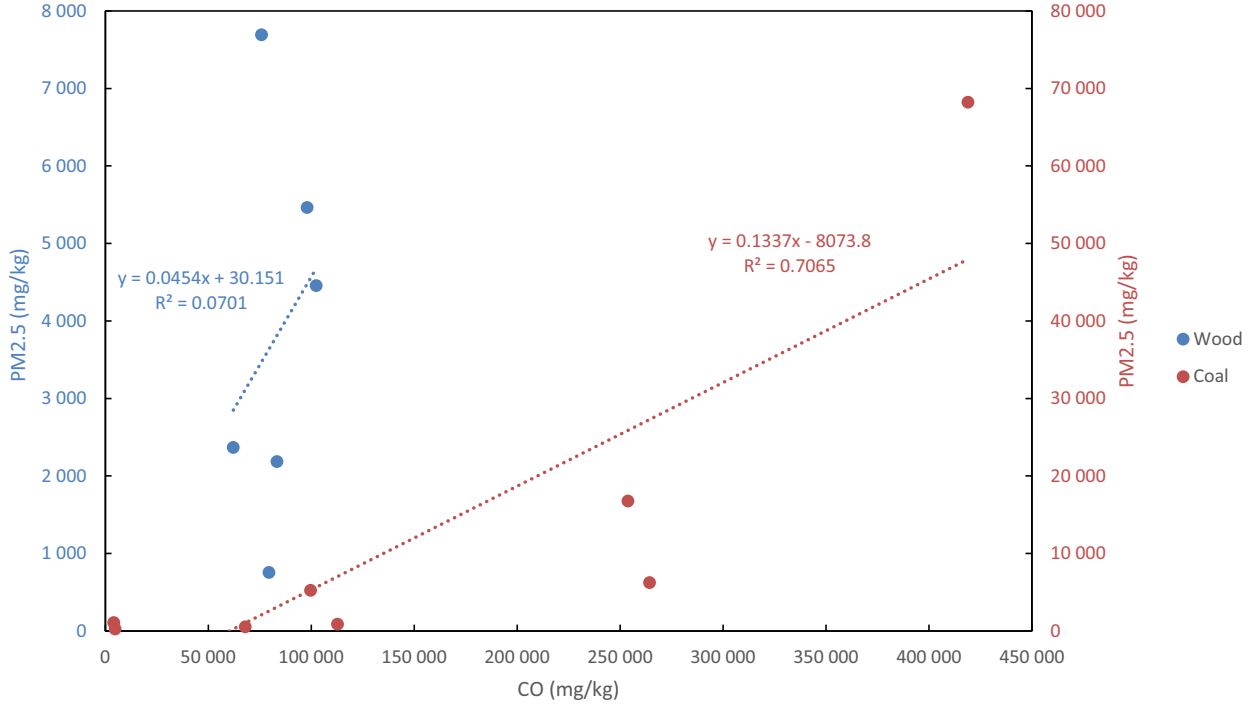

Fig. 3. The correlation between the SE PM2.5 and SE CO.

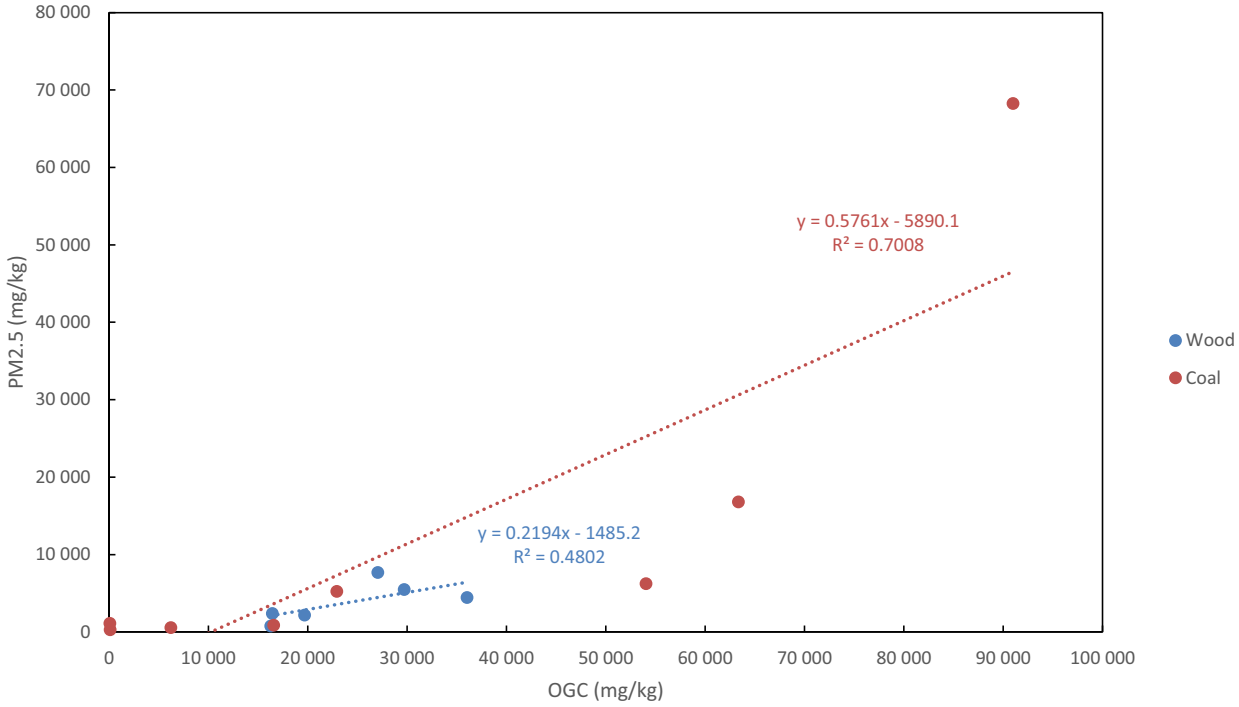

Fig. 4. The correlation of the SE PM2.5 on the SE OGC.

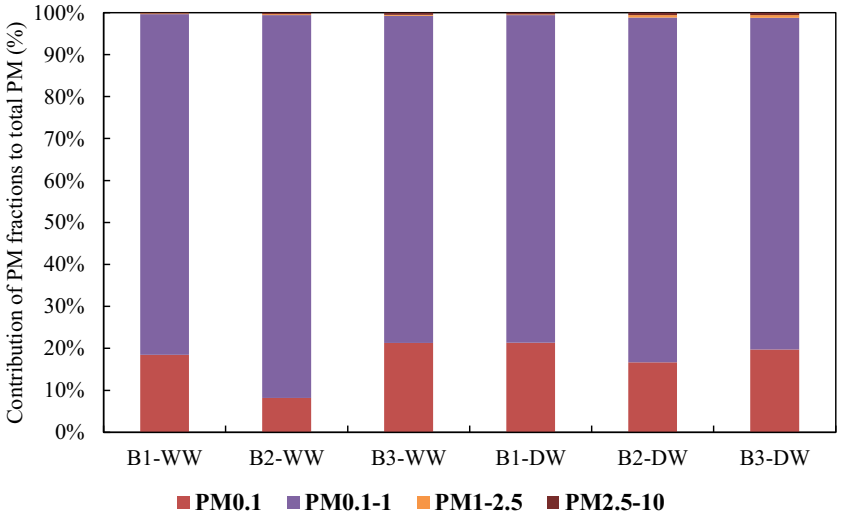

Fig. 5. Particle fractions contributions to PM for biomass combustion.

Understanding these health impacts is crucial for developing public health policies aimed at reducing PM0.1 emissions.

The values in the table are converted to an O_2 concentration of 10 %. The highest numerical concentration of particles <0.1 μm during wood combustion was achieved by boiler B1, while during DW combustion, the average concentration of particles was 6.3×10^{10} #/cm^3. The lowest numerical concentration of particles up to 0.1 μm was measured for boiler B3 during DW combustion and for boiler B2 during WW combustion (approx. 5×10^9 #/cm^3). The highest number of particles with a size of up to 0.8 μm was measured again for boiler B1 during DW combustion – 7.4×10^{10} #/cm^3. The lowest concentration was measured for boiler B3 during combustion of DW at 8×10^9 #/cm^3.

When burning BC, BCB and HC, the highest concentration of particles <0.1 μm was measured for boiler B1 when burning BC1 – 5.6×10^{10} #/cm^3 and the lowest concentration was measured for boiler B4 when burning BC2 and HC2 – 1–1.5 $\times 10^9$ #/cm^3. A similar situation applies to particles up to 0.8 μm in size: the highest concentration of particles was observed for boiler B1 burning BC1 – 6.1×10^{10} #/cm^3, and on the contrary, boiler B4 produced the lowest concentration of particles – approx. 1.8–2 $\times 10^9$ #/cm^3 (both BC2 and HC2 fuel). From the measured data, it can be seen that the lowest number of particles was produced by boiler B4, while the highest was produced by boiler B1.

Figures S1 to S5 show the average particle size number distributions for individual fuels and boilers. The HR-ELPI instrument showed a mostly bimodal distribution of particles, with the first mode at about 18 nm (nucleation mode) and the second at about 40–50 nm (ultrafine mode). During the combustion of HC and WW, an increase in the concentration of particles in the accumulation mode (particle size >100 nm) was also observed.

The presence of these modes indicates a distinct particle formation

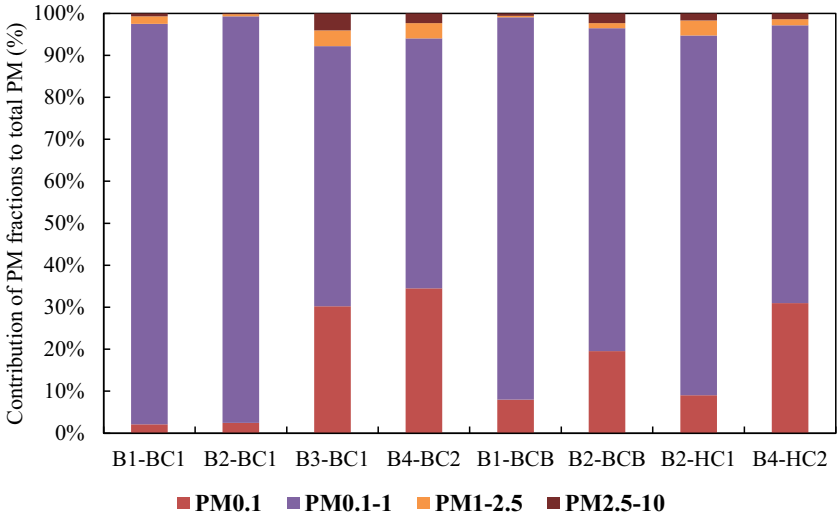

Fig. 6. Particle fractions contributions to PM for coal combustion.

Table 6
Averaged particle number concentration (SMPS).

Test	Particles below 0.1 μm #/cm^3	Particles below 0.8 μm #/cm^3	Ratio between particles below 0.1/0.8 μm
B1-WW	$3.91\times10^{10} \pm 0.90\times10^{10}$	$7.14\times10^{10} \pm 1.64\times10^{10}$	0.55
B2-WW	$4.61\times10^{9} \pm 1.29\times10^{9}$	$1.32\times10^{10} \pm 0.29\times10^{10}$	0.35
B3-WW	$1.94\times10^{10} \pm 0.50\times10^{10}$	$3.65\times10^{10} \pm 0.88\times10^{10}$	0.53
B1-DW	$6.34\times10^{10} \pm 1.59\times10^{10}$	$7.39\times10^{10} \pm 1.77\times10^{10}$	0.86
B2-DW	$3.42\times10^{10} \pm 0.72\times10^{10}$	$3.90\times10^{10} \pm 1.09\times10^{10}$	0.88
B3-DW	$5.66\times10^{9} \pm 1.58\times10^{10}$	$8.02\times10^{9} \pm 1.60\times10^{9}$	0.71
B1-BC1	$5.61\times10^{10} \pm 1.51\times10^{10}$	$6.10\times10^{10} \pm 1.65\times10^{10}$	0.92
B2-BC1	$1.08\times10^{10} \pm 0.30\times10^{10}$	$1.42\times10^{10} \pm 0.38\times10^{10}$	0.76
B3-BC1	$2.79\times10^{10} \pm 0.56\times10^{10}$	$2.92\times10^{10} \pm 0.67\times10^{10}$	0.96
B4-BC2	$1.47\times10^{9} \pm 0.29\times10^{9}$	$1.81\times10^{9} \pm 0.43\times10^{9}$	0.81
B1-BCB	$1.20\times10^{10} \pm 0.34\times10^{10}$	$1.46\times10^{10} \pm 0.39\times10^{10}$	0.82
B2-BCB	$9.52\times10^{9} \pm 2.28\times10^{9}$	$1.06\times10^{10} \pm 0.21\times10^{10}$	0.90
B2-HC1	$6.20\times10^{9} \pm 1.80\times10^{9}$	$9.21\times10^{9} \pm 2.76\times10^{10}$	0.67
B4-HC2	$1.04\times10^{9} \pm 0.30\times10^{9}$	$1.95\times10^{9} \pm 0.43\times10^{9}$	0.53

mechanism, simultaneously occurring in combustion units. Nucleation - dominant in high-temperature zones - leads to new particle formation through two main stages: initial nucleation to create a critical nucleus (overcoming a thermodynamic barrier) and subsequent growth to detectable sizes (overcoming a kinetic barrier via condensation or coagulation). The process of initial particle nucleation in the combustion zone can be simplistically considered under high temperature and oxygen-deficient conditions, where precursors, such as inorganic vapours K, Na, S, collide and chemically react to form initial nuclei [60]. Ultrafine mode particles are suggested to be formed through gas-to-particle conversion, where nucleated clusters grow via condensation of semi-volatile organics, sulfates, and nitrates, as well as coagulation with other small particles. Further coagulation forms accumulation-mode particles, which are most stable and have longer lifetimes, because they are too large for rapid coagulation and too small for efficient gravitational or inertial settling.

Figures S6-S19 show typical trends in particle size and number distributions during combustion tests measured by the HR-ELPI+ instrument. Figure S6 shows the size and number distribution of boiler B3 particles during BC1 combustion. In the first half of the combustion period, a significant amount of particles with a size of 10–60 nm was observed, lasting approximately 2.5 h. The concentration of CO was <2,000 mg/m^3 (converted to O_2=10 %), and the concentration of OGC was <200 mg/m^3. In the second half of the combustion test, the concentration of CO increased to 12,000 mg/m^3 and the concentration of OGC decreased, particles with a size of 10–60 nm were no longer emitted. Particles with a size of 30–110 nm were formed throughout the combustion test. During the combustion of DW (Figure S7), particles in the range of 30–110 nm were again emitted. The formation of particles with a size of 10–60 nm, as in the combustion of BC1, was not observed. During the combustion of WW in boiler B3 (Figure S8), particles in the range of 10–300 nm were formed, while the highest concentrations were reached with sizes of 10–50 nm. The trend of particle formation appeared steady during the combustion test.

The progress of BC1 combustion in boiler B2 is shown in Figure S9. By the middle of the combustion test, CO concentrations>50,000 mg/m^3 and OGC concentrations>15,000 mg/m^3 were measured, accompanied by the formation of particles mainly 100–600 nm in size. As the concentration of CO (<3,000 mg/m^3) and OGC (<500 mg/m^3) decreased, there was a significant formation of particles in the 8–100 nm range, while particles >200 nm were essentially not emitted. The subsequent increase in CO concentration to 8,000–16,000 mg/m^3 (at OGC <500 mg/m^3) was accompanied by the production of particles 30–200 nm in size. During the combustion of HC1 in this boiler (Figure S10), a strong formation of particles with sizes of 10–100 nm was basically not observed. Except for a brief period at the beginning of the test, particles of 100–300 nm were continuously emitted from the head, with a slight shift toward smaller sizes at the end of the test. During the combustion of BCB (Figure S11), the CO concentration fluctuated (3,000–10,000 mg/m^3) in the first half of the combustion test, while the course of the OGC

concentration was relatively stable (<1,000 mg/m^3). In this phase of the combustion process, particles of 10–70 nm were intermittently formed. After that, the CO concentration stabilised at approximately 12,000 mg/m^3 (OGC 2,000–4,000 mg/m^3), and particles in the 10–300 nm size range were produced (they were also measured in the first part of the test). At the end of the test, there was a shift in particle size to the 30–100 nm range (as in the case of HC combustion). During the combustion of WW (Figure S12), a wide spectrum of particles with sizes of 15–700 nm was observed with a maximum at 400 nm. Fuel was added twice during the combustion test (the fuel storage was not large enough for the nearly 5-hour test), but this did not affect the particle characteristics. During the combustion of DW, parts in a wide range of sizes (10–300 nm) were again produced, while the effect of adding fuel is evident by a large increase in the number of particles. Combustion of wood in boiler B2 is accompanied by the production of particles in a significantly wider size spectrum than when burning coal.

The combustion of DW and WW (Figure S14, Figure S15) in boiler B1 is characterised by particles with sizes of 10–800 nm, where the maxima are approximately 20–70 nm (DW) and 10–200 nm (WW). The course of particle formation remains unchanged throughout the combustion test and is accompanied by high concentrations of CO (up to 20,000 mg/m^3) and OGC (up to 10,000 mg/m^3). During the combustion of BC (Figure S16) and BCB (Figure S17), particles with sizes of 30–1000 nm are produced at the beginning of the test (CO concentration up to 80,000 mg/m^3, OGC up to 20,000 mg/m^3), but when the concentration of CO (<8,000 mg/m^3) and OGC (< 1,000 mg/m^3) decreased, in the case of BC1 fuel there is a strong production of particles with a size of 10–100 nm, while particles >300 nm were not detected. This condition lasted essentially until the end of the combustion test. With BCB fuel, the time window for the production of 10–100 nm particles is shorter (approx. 1 hour) and then mainly 30–80 nm particles are produced. Again, particles >300 nm were not detected.

Our temporal HR-ELPI+ data (Figures S6-S19) support this: B1 shows continuous high particle formation throughout the burn cycle, while B3 shows distinct phases correlating with gasification stages.

During the combustion of BC (Figure S18) in boiler B4, mainly particles of 40–110 nm were produced, while the combustion of HC (Figure S19) was characterised by the formation of particles in the 60–110 nm size range with a visible maximum around 105 nm. Due to the stable operation of the boiler, the time graphs of particle size distributions are also stable.

Analysis of the particle size distribution and concentration profiles from individual combustion tests for a given boiler/fuel combination reveals the relationship between the stability of particle size distribution and concentration, and the overall quality and steadiness of the combustion process. Automatic boilers exhibit stable combustion even with smaller fuel inputs, which markedly influences the characteristics of emitted particles, irrespective of the fuel type. In contrast, manually fed boilers show substantial variations in particle emission characteristics depending on the specific phase of the combustion process, with both fuel type and quality exerting a significant effect..

Different boiler designs, among other factors, provide varying residence times in the combustion chamber, leading to significant differences in emissions between boilers. In the boiler B1, the short residence time caused by the direct flame path results in incomplete combustion and high OGC emissions of up to 4,905 mg/MJ with BC1 combustion. In contrast, the boiler B3 extends the residence time through the secondary combustion zone, thereby ensuring a reduction in OGC emissions up to a maximum of 1,637 mg/MJ with WW combustion. The boiler B4 maintains continuous steady-state conditions, ensuring an optimal residence time that enables nearly complete combustion and low OGC emissions below 5 mg/MJ, even when firing BC2.

Considering the effect of boiler designs on atmospheric emissions, the role of secondary air should be mentioned. Our correlation analysis in Fig. 2 argues in favour that secondary air primarily affects the gas-phase oxidation; in contrast, the reduction in PM emissions - supported by the comparatively lower correlation coefficients in Fig. 3 and Fig. 4- can be considered as a secondary, but still significant, effect.

Generally, our results demonstrate that technology replacement provides significant emission reductions: replacing B1 with B4 reduces PM2.5 by 96–99 % regardless of fuel type, and even replacing B1 with an intermediate technology, such as B2, ensures a 70–80 % reduction in pollution. These improvements exceed the performance of add-on control measures, such as electrostatic precipitators, which reduce emissions by 70–90 %, and catalytic converters, which achieve reductions ranging from 25 to 70 %. Therefore, replacing old boiler systems with newer models can be considered efficient and offer environmental benefits similar to those of installing additional gas-cleaning apparatus in older systems.

In this, the specifics of the used fuels should be considered. Thus, wood combustion is characterised by a high volatile content (70–80 %) and requires adequate temperature and mixing. Wet wood (40 % moisture) shows an increase in emissions, associated with a ~200 °C reduction in combustion temperature [61], while water vapour released from combustion material participates in reactions with organic compounds [62]. In contrast, coal combustion is characterised by lower volatile content (30–40 %), but higher ash creates more primary particles [63]. Our research supports this conclusion and, through he strong CO—OGC correlation, indicates that emissions are primarily

4. Conclusions

Small combustion appliances emit a wide range of pollutants that harm human health. The situation is worsened by the fact that most of these appliances are located directly in buildings and, unlike large sources of pollution, do not have any flue gas cleaning system. In addition to common pollutants such as CO, OGC, NO_x, SO_2 and PAHs, these sources also emit dust particles that settle in the respiratory tract. The study aimed to compare the SE of CO, OGC, and PM emitted by old boilers (B1, B2) and more modern boilers (B3, B4) when burning dry wood, wet wood, brown coal, lignite briquettes, and hard coal. The boilers were deliberately operated at a reduced heat output, because older family houses are currently being insulated on a non-negligible scale, but heating systems are often not modernised (e.g. installation of a storage tank so that boilers with manual loading are operated under optimal conditions, i.e. at nominal heat output). The results show that for older-design boilers (B1 and B2), burning wood rather than coal is more advantageous from an emissions perspective. The exception was the combustion of brown coal briquettes (BCB) and brown coal (BC1) in boiler B2, where comparable or lower SE were achieved than when burning wood. SE were higher when burning wet wood than when burning dry wood. The boiler of a more modern design (B3) produced the fewest emissions when burning both wood and brown coal, even with reduced power (flue gas fan switched off). For this boiler, however, no difference was observed in the results between the combustion of wood and brown coal, except for SE OGC, when the brown coal combustion produced approximately 3 times lower SE than that of wood combustion. The automatic boiler (B4), burning both BC and HC, produced significantly lower SE of all monitored pollutants than the other boilers, although the SE were higher than SE from modern wood pellet boilers. Only the gasification boiler (B3) produced a similar level of SE PM2.5 as an automatic boiler. Impactor measurements show that PM1 makes up more than 90 % of the total amount of PM, while the representation of the PM0.1 fraction was about 10–20 % when burning wood and up to 30 % when burning coal. From the point of view of the operation of boilers with manual fueling, these boilers must always be installed with an accumulation tank, when the boilers are operated mainly at nominal heat output, in order to work in the optimal mode and produce the lowest pollutant emissions.

Supplementary Materials

Supplementary Materials

Figure S 1 Averaged particle number size distribution – BC; Figure S 2 Averaged particle number size distribution – BCB; Figure S 3 Averaged particle number size distribution – DW; Figure S 4 Averaged particle number size distribution – HC; Figure S 5 Averaged particle number size distribution – WW; Figure S 6 Particle number size distribution (B3-BC); Figure S 7 Particle number size distribution (B3-DW); Figure S 8 Particle number size distribution (B3-WW); Figure S 9 Particle number size distribution (B2-BC); Figure S 10 Particle number size distribution (B2-HC); Figure S 11 Particle number size distribution (B2-BCB); Figure S 12 Particle number size distribution (B2-WW); Figure S 13 Particle number size distribution (B2-DW); Figure S 14 Particle number size distribution (B1-DW); Figure S 15 Particle number size distribution (B1-WW); Figure S 16 Particle number size distribution (B1-BC); Figure S 17 Particle number size distribution (B1-BCB); Figure S 18 Particle number size distribution (B4-BC); Figure S 19 Particle number size distribution (B4-HC); Table T1 SE of gaseous compounds and particle mass concentrations (WW, DW) – heatmap; Table T2 SE of gaseous compounds and particle mass concentrations (BC, BCB, HC) – heatmap; Table T3 Averaged particle number concentration (SMPS) - heatmap

Funding

This work was financially supported by the European Union under the REFRESH – Research Excellence For Region Sustainability and High-tech Industries project No.CZ.10.03.01/00/22_003/0000048 via the Operational Programme Just Transition.

Data availability

The raw data supporting the conclusions of this article will be made available by the authors on request.

Conflicts of interest

The authors declare no conflicts of interest.

CRediT authorship contribution statement

Kamil Krpec: Writing – review & editing, Writing – original draft, Visualization, Methodology, Investigation, Formal analysis, Data curation, Conceptualization. **Oleksandr Molchanov:** Writing – review & editing, Methodology. **Lenka Kuboňová:** Writing – original draft. **Jenn-Kun Kuo:** Writing – review & editing.

Declaration of competing interest

The authors declare that they have no known competing financial interests or personal relationships that could have appeared to influence the work reported in this paper.

Acknowledgments

We would like to thank the project LIFE-IP SK AQ Improvement (LIFE18 IPE/SK/000010).

Supplementary materials

Supplementary material associated with this article can be found, in the online version, at doi:10.1016/j.jaecs.2025.100441.

References

[1] EEA, European environment agency, air pollutant emissions data viewer (Gothenburg protocol, LRTAP convention) 1990-2018. Available at:, 2021.
[2] CHMI, Graphic yearbook. Available at: http://portal.chmi.cz/files/portal/docs/uoco/isko/grafroc/17groc/gr17cz/IV1_PM_CZ.html, 2017.
[3] P. Machálek, J. Machart, Upravená emisní bilance vytápění bytů malými zdroji od roku 2006 (translation to English: modified emission balance of appartments heating by small-scale units from the year 2006), Milevsko, 2007.
[4] McDuffie E, Martin R, Spadaro J, Burnett R, Smith S, O'Rourke P, Hammer M, van Donkelaar A, Bindle L, Shah V, Jaeglé L, Luo G, Yu F, Adeniran J, Lin J, Brauer M. Source sector and fuel contributions to ambient $PM_{2.5}$and attributable mortality across multiple spatial scales.] Nat Commun 2021.
[5] Winijkul E, Bond T. Emissions from residential combustion considering end-uses and spatial constraints: part II, emission reduction scenarios]. Atmos. Environ. 2016:1–11.
[6] Simoneit B. Biomass burning - A review of organic tracers for smoke from incomplete combustion.] Appl Geochem 2002:129–62.
[7] van Pinxteren D, Engelhardt V, Mothes F, Poulain L, Fomba K, Spindler G, Cuesta-Mosquera A, Tuch T, Müller T, Wiedensohler A, Löschau G, Bastian S, Herrmann H. Residential wood combustion in Germany: a twin-site study of local village contributions to particulate pollutants and their potential health effects.] ACS Environ Au 2023:12–30.
[8] Thomas R. Particle size and pathogenicity in the respiratory tract.] Virulence 2013:847–58.
[9] Sugita K, Goto S, Endo O, Nakajima D, Yajima H, Ishii T. Particle size effects on the deposition ratios of airborne particles in the respiratory tract.] J Health Sci 2004:185–8.
[10] Cheng Y, Yu H, Xie S, Zhao J, Ye Y. Study on the coal dust deposition fraction and site in the upper respiratory tract under different particle sizes and labor intensities]. Sci Total Environ 2023.
[11] Tissari J, Hytonen K, Sippula O, Jokiniemi J. The effects of operating conditions on emissions from masonry heaters and sauna stoves. Biomass Bioenergy 2009;33:513–20.
[12] Brandelet B, Rose C, Rogaume C, Rogaume Y. Impact of ignition technique on total emissions of a firewood stove.] Biomass Bioenergy 2018:15–24.
[13] Reichert G, Schmidl C, Haslinger W, Schwabl M, Moser W, Aigenbauer S, Wohler M, Hochenauer C. Investigation of user behavior and assessment of typical operation mode for different types of firewood room heating appliances in Austria. Renew Energy 2016;93:245–54.
[14] Wohler M, Andersen JS, Becker G, Persson H, Reichert G, Schon C, Schmidl C, Jaeger D, Pelz SK. Investigation of real life operation of biomass room heating appliances - results of a European survey. Appl Energy 2016;169:240–9.
[15] Tissari J, Hytönen K, Lyyränen J, Jokiniemi J. A novel field measurement method for determining fine particle and gas emissions from residential wood combustion. Atmos Environ 2007;41:8330–44.
[16] Martiník L, Drastichová V, Horák J, Jankovská Z, Krpec K, Kubesa P, Hopan F, Kaličáková Z. Spalováni odpadní biomasy v malých zařízeních (translation to English: the combustion of waste biomass in small-scale combustion units). Chemické listy 2014;108:156–62.
[17] O. Sippula, Fine particle formation and emission in biomass combustion, Department of Environmental Science, University of Eastern Finland, Finland, 2010.
[18] I. Obernberger, T. Brunner, G. Barnthaler, Fine particle emissions from modern Austrian small scale biomass combustion plants, 15th European biomass conference and exhibitionGermany, 2007.
[19] Johansson LS, Leckner B, Gustavsson L, Cooper D, Tullin C, Potter A. Emission characteristics of modern and old-type residential boilers fired with wood logs and wood pellets. Atmos Environ 2004;38:4183–95.
[20] Kraszkiewicz A. The combustion of wood biomass in low power coal-fired boilers. Combust Sci Technol 2016;188:389–96.
[21] Molchanov O, Krpec K, Horák J, Kubonová L, Hopan F, Rysavy J. Combined control of PM and NOx emissions from small-scale combustions by electrostatic precipitation. Res Eng 2024;24.
[22] Molchanov O, Krpec K, Horák J, Kubonová L, Hopan F, Rysavy J. Application end evaluation of electrostatic precipitation for control PM and NOx emissions from small-scale combustions. Fire-Switzerland 2024;7.
[23] Rysavy J, Vicente E, Jaroch M, Alves C, de la Campa A, Horák J. Reducing the impact of biomass combustion in residential units on local air quality by using innovative low-loading Pt-based heterogeneous catalyst. Biomass Bioenergy 2024;183.
[24] Rysavy J, Serencísová J, Horák J, Ochodek T. The co-combustion of pellets with pistachio shells in residential units additionally equipped by Pt-based catalyst. Biomass Convers Biorefin 2023;13:16511–27.
[25] Szramowiat-Sala K, Penkala R, Horák J, Krpec K, Hopan F, Rysavy J, Borovec K, Górecki J. AI-based data mining approach to control the environmental impact of conventional energy technologies. J Clean Prod 2024;472.
[26] Mack R, Schön C, Kuptz D, Hartmann H, Brunner T, Obernberger I, Behr H. Influence of wood species and additives on emission behavior of wood pellets in a residential pellet stove and a boiler.] Biomass Convers Biorefin 2023.
[27] Křůmal K, Mikuška P, Horák J, Hopan F, Krpec K. Comparison of emissions of gaseous and particulate pollutants from the combustion of biomass and coal in modern and old-type boilers used for residential heating in the Czech Republic, Central Europe. Chemosphere 2019;229:51–9.
[28] ISO, Solid biofuels – Determination of moisture content – Oven dry method – Part 2: total moisture – Simplified method, ISO 18134-2:2017, 2017, pp. 12.

[29] ISO, Solid mineral fuels - determination of ash, 2010.
[30] ISO, Solid biofuels – determination of ash content, ISO 18122:2015, 2015, pp. 12.
[31] ISO, Solid mineral fuels – determination of total carbon, hydrogen and nitrogen content – Instrumental method, International Organization for Standardization, 2010, pp. 10.
[32] ISO, Solid biofuels — determination of total content of carbon, hydrogen and nitrogen, International Organization for Standardization, 2015, pp. 9.
[33] ISO, Solid mineral fuels – determination of sulphur by IR spectrometry, ISO 19579: 2006, 2006, pp. 4.
[34] ISO, Solid biofuels - determination of total content of sulfur and chlorine, 2016.
[35] ISO, Solid mineral fuels - determination of gross calorific value by the bomb calorimetric method, and calculation of net calorific value, 2010.
[36] ISO, Solid biofuels - determination of calorific value, 2017.
[37] EPA, Method 5G - particulate matter wood heaters from a dilution tunnel, 2017.
[38] Horák J, Laciok V, Krpec K, Hopan F, Dej M, Kubesa P, Rysavy J, Molchanov O, Kubonová L. Influence of the type and output of domestic hot-water boilers and wood moisture on the production of fine and ultrafine particulate matter. Atmos Environ 2020:229.
[39] Biswas P, Flagan RC. High-velocity inertial impactors. Environ Sci Technol 1984; 18:611–6.
[40] Wang C, Seames WS, Gadgil M, Hrdlicka J, Fix G. Comparison of coal ash particle size distributions from Berner and Dekati low pressure impactors. Aerosol Sci Technol 2007;41:1049–62.
[41] CEN, Heating boilers – part 5: heating boilers for solid fuels, manually and automatically stoked, nominal heat output of up to 500 kW – terminology, requirements, testing and marking, European Committee for Standardization, 2012.
[42] Kraszkiewicz A, Przywara A, Anifantis AS. Impact of ignition technique on pollutants emission during the combustion of selected solid biofuels. Energies (Basel) 2020:13.
[43] Orszulik E, Sliwinska A. Combustion of hard coal and alternative fuels in a boiler with an innovative retort burner. Combust Sci Technol 2019;191:555–69.
[44] Pelka G, Jach-Nocon M, Paprocki M, Jachimowski A, Lubon W, Nocon A, Wygoda M, Wyczesany P, Pachytel P, Mirowski T. Comparison of emissions and efficiency of two types of burners when burning wood pellets from different suppliers. Energies (Basel) 2023.
[45] Nussbaumer T, Lauber A. Formation mechanism and physical properties of particles from wood combustion for design and operation of electrostatic precipitators. 18th Euro Biomass Conf Exhib 2010;113:3–7.
[46] Nussbaumer T. Combustion and Co-combustion of biomass: fundamentals, technologies, and primary measures for emission reduction. Energy Fuels 2003;17: 1510–21.
[47] Knigawka P, Pianko-Oprych P, Krpec K, Kubonová L. Comparison of emissions from smokeless coal combustion in a household heating boiler used in Central Europe. Int J Environ Sci Technol 2022;19:7151–64.
[48] Rysavy J, Horak J, Hopan F, Kubonová L, Krpec K, Molchanov O, Garba M, Ochodek T. Influence of flue gas parameters on conversion rates of honeycomb catalysts. Sep Purif Technol 2022;278.
[49] Meyer NK. Particulate, black carbon and organic emissions from small-scale residential wood combustion appliances in Switzerland. Biomass Bioenergy 2012; 36:31–42.
[50] Uski O, Jalava PI, Happo MS, Leskinen J, Sippula O, Tissari J, Mäki-Paakkanen J, Jokiniemi J, Hirvonen MR. Different toxic mechanisms are activated by emission PM depending on combustion efficiency. Atmos Environ 2014;89:623–32.
[51] Bari MA, Baumbach G, Brodbeck J, Struschka M, Kuch B, Dreher W, Scheffknecht G. Characterisation of particulates and carcinogenic polycyclic aromatic hydrocarbons in wintertime wood-fired heating in residential areas. Atmos Environ 2011;45:7627–34.
[52] Boman C, Nordin A, Boström D, Öhman M. Characterization of inorganic particulate matter from residential combustion of pelletized biomass fuels. Energy Fuels 2004;18:338–48.
[53] Obaidullah M, Bram S, Verma VK, De Ruyck J. A review on particle emissions from small scale biomass combustion. Int J Renew Energy Technol 2012;2:147–59.
[54] Leskinen J, Tissari J, Uski O, Viren A, Torvela T, Kaivosoja T, Lamberg H, Nuutinen I, Kettunen T, Joutsensaari J, Jalava PI, Sippula O, Hirvonen MR, Jokiniemi J. Fine particle emissions in three different combustion conditions of a wood chip-fired appliance particulate physico-chemical properties and induced cell death. Atmos Environ 2014;86:129–39.
[55] Landrigan P, Fuller R, Acosta N. The Lancet Commission on pollution and health (vol 391, pg 463, 2018). Lancet 2018;391. 430-430.
[56] Fattore E, Paiano V, Borgini A, Tittarelli A, Bertoldi M, Crosignani P, Fanelli R. Human health risk in relation to air quality in two municipalities in an industrialized area of Northern Italy. Environ Res 2011;111:1321–7.
[57] Shen G, Tao S, Chen Y, Zhang Y, Wei S, Xue M, Wang B, Wang R, Lu Y, Li W, Shen H, Huang Y, Chen H. Emission characteristics for polycyclic aromatic hydrocarbons from solid fuels burned in domestic stoves in rural China. Environ Sci Technol 2013;47:14485–94.
[58] Samae H, Tekasakul S, Tekasakul P, Furuuchi M. Emission factors of ultrafine particulate matter (PM<0.1 μm) and particle-bound polycyclic aromatic hydrocarbons from biomass combustion for source apportionment. Chemosphere 2021;262.
[59] Sikorova J, Hopan F, Kubonova L, Horak J, Milcova A, Rossner P, Ambroz A, Krpec K, Molchanov O, Zavodna T. The genotoxic potential of organic emissions from domestic boilers combusting biomass and fossil fuels. Toxics 2025;13.
[60] Lv JY, Ren XD, Gao J. A modeling study on the nucleation, growth and coagulation of soot particles in combustion flame. Adv Mat Res 2014;953-954:1167–70.
[61] Tucho B, Etefa H, Kumar V, Raba G, Efa M, Dejene F. Effect of wood moisture content on the performance of wood burning cook stoves. Int J Sustain Eng 2023; 16:1–10.
[62] T. Le Cong, P. Dagaut, Effect of water vapor on the kinetics of combustion of hydrogen and natural gas: experimental and detailed modeling study, 2008, pp. 319–28.
[63] Zhang Y, Yuan Q, Huang D, Kong S, Zhang J, Wang X, Lu C, Shi Z, Zhang X, Sun Y, Wang Z, Shao L, Zhu J, Li W. Direct observations of fine primary particles from residential coal burning: insights into their morphology, composition, and hygroscopicity. J Geophys Res: Atmos 2018;123. 12,964-912,979.